Redox Biology 70 (2024) 103085

Contents lists available at ScienceDirect

Redox Biology

journal homepage: www.elsevier.com/locate/redox

Neurogranin expression regulates mitochondrial function and redox balance in endothelial cells

Ashton N. Jorgensen [a], Nabil A. Rashdan [b], K.N. Shashanka Rao [c], Luisa F. Delgadillo [b], Gopi K. Kolluru [d], David M. Krzywanski [c], Christopher B. Pattillo [b], Christopher G. Kevil [d], Hyung W. Nam [a,*]

[a] Department of Pharmacology, Toxicology, and Neuroscience, Louisiana State University Health Sciences Center, Shreveport, LA, 71103, USA
[b] Department of Molecular and Cellular Physiology, Louisiana State University Health Sciences Center, Shreveport, LA, 71103, USA
[c] Department of Cellular Biology and Anatomy, Louisiana State University Health Sciences Center, Shreveport, LA, 71103, USA
[d] Department of Pathology, Louisiana State University Health Sciences Center, Shreveport, LA, 71103, USA

ARTICLE INFO

Keywords:
Reactive oxygen species
Mitochondria
MitoEbselen
Hydrogen peroxide
Neurogranin

ABSTRACT

Endothelial dysfunction and endothelial activation are common early events in vascular diseases and can arise from mitochondrial dysfunction. Neurogranin (Ng) is a 17kD protein well known to regulate intracellular Ca^{2+}-calmodulin (CaM) complex signaling, and its dysfunction is significantly implicated in brain aging and neurodegenerative diseases. We found that Ng is also expressed in human aortic endothelial cells (HAECs), and depleting Ng promotes Ca^{2+}-CaM complex-dependent endothelial activation and redox imbalances. Endothelial-specific Ng knockout (Cre-CDH5-$Ng^{f/f}$) mice demonstrate a significant delay in the flow-mediated dilation (FMD) response. Therefore, it is critical to characterize how endothelial Ng expression regulates reactive oxygen species (ROS) generation and affects cardiovascular disease. Label-free quantification proteomics identified that mitochondrial dysfunction and the oxidative phosphorylation pathway are significantly changed in the aorta of Cre-CDH5-$Ng^{f/f}$ mice. We found that a significant amount of Ng is expressed in the mitochondrial fraction of HAECs using western blotting and colocalized with the mitochondrial marker, COX IV, using immunofluorescence staining. Seahorse assay demonstrated that a lack of Ng decreases mitochondrial respiration. Treatment with MitoEbselen significantly restores the oxygen consumption rate in Ng knockdown cells. With the RoGFP-Orp1 approach, we identified that Ng knockdown increases mitochondrial-specific hydrogen peroxide (H_2O_2) production, and MitoEbselen treatment significantly reduced mitochondrial ROS (mtROS) levels in Ng knockdown cells. These results suggest that Ng plays a significant role in mtROS production. We discovered that MitoEbselen treatment also rescues decreased eNOS expression and nitric oxide (NO) levels in Ng knockdown cells, which implicates the critical role of Ng in mtROS-NO balance in the endothelial cells.

1. Introduction

The interplay between nitric oxide (NO) and reactive oxygen species (ROS) is crucial to the preservation of vascular homeostasis. Imbalances in the production of NO and ROS, superoxide ($O_2^{\bullet-}$) and H_2O_2, are strongly associated with endothelial dysfunction and the development of cardiovascular disease (CVD) [1,2]. NO is a potent vasodilator and regulates various physiological processes, including blood pressure, platelet function, and inflammation. Endothelial dysfunction is described as the impairment of endothelium-dependent vasodilation, which signifies reduced availability of vascular NO generated by endothelial NO synthase (eNOS). This decrease in NO can occur due to increased ROS production and eNOS uncoupling induced by mitochondrial dysfunction [3–5].

Although mitochondria are most known for their significance in ATP production, they participate in several other biological processes, including cell death, calcium signaling, and generation of ROS [6]. The main function of mitochondria within endothelial cells is considered to be regulation of mtROS production in response to environmental cues [7–9]. mtROS are usually generated as byproducts of oxidative phosphorylation. $O_2^{\bullet-}$ produced by complex I and III of the electron transport chain will be readily converted into H_2O_2 by superoxide dismutase

* Corresponding author.
E-mail address: hyung.nam@lsuhs.edu (H.W. Nam).

https://doi.org/10.1016/j.redox.2024.103085
Received 20 January 2024; Received in revised form 8 February 2024; Accepted 10 February 2024
Available online 11 February 2024

(SOD) and then to O_2 and H_2O_2 by glutathione peroxidase (GPx) or catalase [10]. Ca^{2+} signaling in endothelial cells can influence mtROS production via oxidative phosphorylation and increases in intracellular calcium levels can activate several mitochondrial antioxidant enzymes such as SOD and catalase, which are beneficial to the vascular health [11]. Thus, Ca^{2+} signaling associated with mitochondrial function must be tightly regulated for proper redox balance within endothelial cells. However, mechanisms of Ca^{2+}-mediated mtROS production during the pathogenesis of CVD are not well understood.

While transient increases in ROS are important for physiological cellular signaling events, prolonged increases can cause oxidative stress and inflammatory cell states, which are known to both promote and be induced by several CVD [12–14]. There are numerous ways ROS can influence the vasculature, with the most noticeable being the ability of $O_2^{\bullet-}$ to react directly with NO to form of peroxynitrite ($ONOO^-$) that can further contribute to eNOS uncoupling in a snowball effect [5,15]. H_2O_2 can diffuse freely between cell membranes and while small increases induce vasodilation, high concentrations of H_2O_2 are seen to cause vasoconstriction [16]. Disrupted calcium homeostasis can contribute to the dysregulation of both NO and ROS generation and their downstream events [17]. Therefore, understanding the intricate interplay between Ca^{2+}, NO, and mtROS is crucial for developing targeted therapies to improve cardiovascular health.

Neurogranin (Ng) is a Ca^{2+} sensing protein known to regulate intracellular Ca^{2+}-CaM formation and downstream signaling in neurons [18,19]. Under low intracellular Ca^{2+} conditions, Ng demonstrates a strong affinity for apo-CaM, which results in Ng-mediated inhibition of Ca^{2+}-CaM complex formation [20,21]. In turn, PKCγ-dependent phosphorylation of the CaM-binding sites of Ng (S37) regulates Ng-CaM binding affinity [19,22]. S-nitrosylation of Ng renders it a highly favorable acceptor of NO modification at four Cys residues, which leads to dramatically attenuated CaM binding affinity and 2-fold weaker PKC substrate phosphorylation activity [18,19]. Overall, cellular Ng expression plays a critical role in Ca^{2+} sensing in response to PKC activity and affects downstream Ca^{2+}-CaM-dependent kinase II (CaMKII) and calcineurin (CaN) activation.

Although Ng is known as a brain-specific protein and impacts the pathophysiology of several neurological diseases [23–25], Ng can also be expressed outside of the brain. Recent studies have demonstrated that Ng plays an important role in Ca^{2+} signaling in T-cells [23], skeletal muscle [24], and cardiomyocytes [25]. Furthermore, a previous study indicated that depletion of Ng expression in the human aortic endothelial cell reduces NO bioavailability by inhibiting eNOS activity, suppresses AKT activation during shear stress, and ultimately induces endothelial dysfunction [26]. Therefore, it is important to further characterize the role of Ng expression in the endothelium, as it may be related to the pathophysiology of CVD.

Interestingly, previous neuropathology studies revealed Ng-immunoreactivity at the membranes of both the mitochondria and trans-Golgi vesicles in neurons [27]. These are areas critical for mtROS and NO production, which suggests Ng may play a role in these functions. Here, we report that Ng is uniquely expressed in the mitochondria of human endothelial cells. Using label-free quantification proteomics, we found that mitochondrial dysfunction and oxidative phosphorylation are significantly changed in the aorta of Cre-CDH5-$Ng^{f/f}$ mice. These mice also display endothelial dysfunction after flow-mediated dilation measurements. Therefore, we hypothesized that Ng expression plays an important role in mitochondrial function and mtROS production that influences NO availability in endothelial cells. With *in vitro* experiments using HAECs, we found that Ng expression levels affect mitochondrial respiration, ATP production, and mtROS production. Mitochondrial antioxidant treatment selectively restores mtROS and eNOS dysregulation observed in Ng knockdown cells. These findings suggest that Ng expression impacts mitochondrial respiration and mtROS generation in HAECs, which ultimately influences NO production. Overall, this study provides a new understanding of the regulation and relationship between mtROS and NO production in the endothelium.

2. Materials and methods

2.1. Animals

Male endothelial-specific Ng knockout Cre-CDH5-$Ng^{f/f}$ and control $Ng^{f/f}$ mice (C57BL/6J background, Cyagene) aged 4-month-old were used. Mice were group-housed in standard Plexiglas cages under a 12 h light/dark cycle (lights on at 6:00 a.m.) at a constant temperature (24 ± 0.5 °C) and humidity (60 ± 2%) with food and water available *ad libitum*. The animal care and handling procedures were in accordance with LSUHSC institutional and National Institutes of Health (NIH) guidelines.

2.2. Flow-mediated vasodilation and transthoracic echocardiography

Using high-frequency ultrasound, we measured endothelium-dependent dilation of the femoral artery after temporal ischemia of the lower part of the hindlimb in control and endothelial-specific Ng knockout mice [28]. The ultrasound probe was attached to a stereotactic holder and manually aligned with the femoral vein visible at the upper inner thigh. A vascular occlude (5 mm diameter, Harvard Apparatus) was placed around the proximal hindlimb to induce occlusion of the distal hindlimb as an ischemic trigger. Following hindlimb ischemia for 1 min, the cuff was deflated, and femoral artery diameter measurements were continuously recorded for 5 min at 30-sec intervals. Using a Visual Sonics Vevo 3100 imaging system, two-dimensional and motion-mode (Mmode) transthoracic echocardiography was performed in both control and endothelial-specific Ng knockout mice. Mice were anesthetized with isoflurane gas, and the physiological response of the heart was assessed as previously described by Ref. [29]. Off-line analyses included measurement in diastole of the interventricular septum (IVS_d) and left ventricular free wall ($LVFW_d$) thickness and the left ventricular (LV) end-diastolic and end-systolic internal dimensions ($LVID_d$ and $LVID_s$, respectively). LV shortening fraction (SF) was calculated as $SF = ((LVID_d - LVID_s)/LVID_d) \times 100$.

2.3. Cell culture and treatments

Primary HAECs (#PCS-100-011, ATCC) were purchased and maintained in MCDB 131 medium supplemented with 10% fetal bovine serum (FBS), 2 mmol/L glutamax, 10 U/mL penicillin, 100 μg/ml streptomycin (GIBCO/Life Technologies), 30 μg/ml heparin sodium, and bovine brain extract (25 μg/ml). For Ng knockdown and overexpression, HAECs at 70% confluency were transfected with siRNA (20 pmol, #s9723, Thermo Fisher) or plasmid DNA vector targeting Ng overexpression with an HA tag (2 μmol, VectorBuilder ID #VB211018-1249cnr), respectively, using Lipofectamine RNAiMAX (#13778150, Thermo Fisher) for 8 h. Cells were then switched to growth media and experiments performed 24 h later. When applicable, before experiments, transfected cells were treated with 1 nmol MitoEbselen-2 (#564356, MedKoo Biosciences) in reduced-serum media for 30 min.

2.4. Subcellular fractionation and western blot analysis

Control HAECs were separated into cytosolic, membrane, soluble nuclear, chromatin-bound nuclear, and cytoskeletal fractions using the Pierce Subcellular Protein Fractionation Kit for cultured cells (Thermo Scientific, #78840). A set of transfected HAECs were separated into cytosolic and mitochondrial lysates using the Mitochondria/Cytosol Fractionation Kit (Abcam, #ab65320). Protein concentration was quantified using the Pierce™ BCA Protein Assay Kit (Thermo Fisher) and samples prepped for Western blot. Proteins were separated using 4–12% SDS-PAGE (BioRad) at 100 V for 1.5 h, transferred onto PVDF membranes at 25 V for 7 min using a Trans-Blot Turbo Transfer System (BioRad), and incubated with antibodies against Neurogranin #07–425-

I (Millipore), Calmodulin #35944, COX IV #4850T, eNOS #32027S, and Phospho-eNOS (S1177) #9570 (Cell Signaling), and GAPDH #SC-32233 (Santa Cruz). Chemiluminescent bands were detected on a Bio-Rad ChemiDoc™ MP Imaging System and quantified using NIH Image J software.

2.5. Immunofluorescence

For immunofluorescence staining, control HAECs were cultured in 24-well plates on coverslips until 70% confluency. Then, they were fixed with 2% formaldehyde, permeabilized with 0.2% Triton X-100, and blocked in 1% BSA with azide. Primary antibodies for Neurogranin (#07–425-1, Millipore), eNOS (#ab76198, Abcam), Calmodulin (#MA3–917, Invitrogen), and COX IV (#ab33985, Abcam) were incubated overnight followed by staining with Alexa Fluor-conjugated secondary antibodies (Cell Signaling). Coverslips were then mounted with Prolong™ Diamond Antifade Mountant with DAPI (#P36971, Invitrogen) and allowed to cure for 24 h. Fluorescence was quantified using ImageJ and calculated as corrected total cell fluorescence [(CTCF) = integrated density – (area of selected cell x mean fluorescence of background readings)] and normalized to control levels.

2.6. Oxygen consumption rate (OCR) measurements

To assess mitochondrial function in HAECs, OCR was measured using a Seahorse Bioscience XF24 extracellular flux analyzer. For these experiments, transfected HAECs were seeded at 100,000 cells per well onto Seahorse Bioscience V7 tissue culture plates in growth media. Cells were allowed to adhere and grow for 6 h, then the growth media was changed to reduced-serum media. One hour before the start of the extracellular flux assay, the media was changed to serum-free Dulbecco's Modified Eagle Medicum (DMEM) supplemented with 25 mmol/L D-glucose, 2 mmoL/L L-glutamine, and 1 mmol/L pyruvate. The pH of the medium was adjusted to 7.4 with NaOH. Where indicated, the following were injected through ports in the Seahorse Flux Pak cartridges: ATP-synthesis inhibitor oligomycin (1 μg/ml), carbonyl cyanide 4-(trifluoromethoxy) phenylhydrazone (FCCP; 1 μmol/L) to uncouple ATP synthesis, rotenone (1 μmol/L) to block complex I, and antimycin A (10 μmol/L) (Sigma) to block complex III. Basal ECAR, OCR, and spare respiratory capacity were generated by Wave Desktop software (Agilent Technologies). To allow comparison between experiments, data are expressed as the OCR in pmol/min/μg protein. OCR is represented by the total OCR of the cells before addition of mitochondrial inhibitors. Because oligomycin inhibits mitochondrial ATP synthase (complex V), non-ATP–linked OCR is equal to the rate observed in the presence of oligomycin. Consequently, ATP-linked OCR is determined by subtracting the non-ATP OCR from the baseline OCR. Maximal OCR is determined in the presence of FCCP, an ionophore that collapses the inner membrane gradient of the electron transport chain, leading to maximal oxygen consumption to re-establish a membrane potential. Finally, addition of antimycin A and rotenone blocks electron entry into the electron transport chain, inhibiting mitochondrial oxygen consumption.

2.7. Mito-roGFP2-Orp1 Telo-HAEC cell culture

293T cells were maintained in high glucose DMEM supplemented with 10% FBS and 1% antibiotic-antimycotic. Cells were grown in 10 cm dishes to ~60% confluence and transfected with 2 μg pMD2.G, 5 μg pGAG/pol, and 10 μg pLPCX mito-roGFP2-Orp1 using Lipofectamine 3000. Cell culture media was changed to antibiotic-free media the next day. Media was then changed daily for 2 days, collected, and pooled. Pooled viral supernatant was centrifuged at 500 g for 10 min, filtered through a 0.45 μm PES syringe filter, aliquoted, and stored at −80 °C until further use.

An hTERT immortalized HAEC cell line (Telo-HAEC) was purchased from ATCC and maintained in endothelial growth media (EGM) containing OptiMEM supplemented with sodium bicarbonate (2.4 g/L), fetal bovine serum (5% v/v), bovine brain extract (0.25% v/v), Gentamicin sulfate (50 μg/ml), amphotericin (250 ng/ml), epidermal growth factor (10 ng/ml), Heparin sulfate (90 μg/ml), and hydrocortisone (1 μg/ml). All experiments were performed between passages 5 and 7. Telo-HAECs at ~50% confluence in a 6-well plate were cultured in 2 ml of viral supernatant supplemented with 8 μg/ml polybrene for 48 h. Transfected Telo-HAECs were split into 10 cm dishes and grown to confluency. Cells were then sorted using a Bigfoot fluorescence-activated cell sorting machine and selected for double positive for BV510 and FITC as mito-Orp1 expressing cells.

2.8. Mitochondrial-hydrogen peroxide measurements

Telo-HAECs stably expressing the mito-Orp1 sensor were transfected with siRNA or plasmid DNA targeting Ng knockdown and overexpression, respectively. Cells were then seeded at 10^3 cells/well in a coverslip glass-bottomed 96-well plate (#P96-1.5 P, Celvis) and allowed to attach overnight. A set of wells under each condition was pretreated with MitoEbselen for 20 min. Images were taken using a Nikon Eclipse Ti2 inverted microscope where Mito-Orp1 was excited sequentially using an X-cite-120 xenon lamp with either a 395/25 nm filter or 480/20 nm excitation filter passing through a 505 nm dichroic mirror, while a 510/20 nm emission filter was used for detection. Baseline images were taken for 5 min. Then, a separate well under each condition was treated with 1 mM of DTT, DMD, or left untreated and imaged for 20 min. The ratio of fluorescent intensity for each well at 395nm/480 nm was analyzed using NIS Elements AR5. Data is presented as the normalized ratio of oxidized mito-Orp1 to reduced mito-Orp1 calculated as (F–Fmin)/(Fmax–Fmin) where F is the fluorescence intensity measured from wells. Fmin refers to the fluorescence intensity after addition of 1 mM DTT (promotes maximal mito-Orp1 reduction, i.e., inhibits H_2O_2 interaction with mito-Orp1), taken as 0%. Fmax is the fluorescence measured after addition of 1 mM DMD (a thiol-specific oxidant, completely oxidizing the Orp1 thiol peroxidase), taken as 100%.

2.9. Superoxide measurements

Endothelial $O_2^{\bullet-}$ production was measured using the hydroethidine (HE) reverse-phase high-performance liquid chromatography (HPLC) method, as previously described [30]. Briefly, cells were incubated with low-serum media containing 10 μM HE for 30 min. A 1 nM MitoEbselen-2 treatment group was also included. Cells were then washed with ice-cold PBS, pelleted, and lysed with Triton X-100. Proteins were precipitated using acidified methanol and 2-OH-ethidium (2-OH-E+) enriched using a microcolumn preparation of Dowex 50WX-8 cation exchange resin and eluted with 10 N HCl. 2-OH-E+ product was measured using fluorescence detection (excitation 490 nm; emission 567 nm) with a Shimadzu HPLC system (Shimadzu Corporation). 2-OH-E + concentration was normalized to total protein. Peaks for both the parent HE and (2-OH-E+) were detected in all HPLC runs ensuring that the HE was not exhausted during $O_2^{\bullet-}$ detection.

2.10. Nitric oxide measurements

Nitric oxide was measured using a Sievers Nitric Oxide Analyzer 280i in the COBRE Redox Molecular Signaling Core at LSUHS Shreveport. Briefly, cell pellets were washed with ice-cold PBS and resuspended in NO stabilization buffer (800 mM potassium ferricyanide, 17.6 mM N-ethylmaleimide, 6% Nonidet P-40) for analysis. NO was then measured using an ozone-based chemiluminescent assay, previously explained [31]. Aliquots of samples were tested for sulfanilamide resistance following the addition of an acidic sulfanilamide solution to a final concentration of 0.5% v/v and sitting in the dark for 15 min prior to injection into the analyzer. NO levels were then normalized to the

protein concentration of the samples.

2.11. Aorta tissue sample preparation

$Ng^{f/f}$ mice (n = 4) and Cre-CDH5-$Ng^{f/f}$ mice (n = 5) were subjected to isoflurane gas to induce unconsciousness, followed by PBS perfusion and isolation of the aorta. The extracted tissue was snap-frozen on dry ice and stored at −80 °C until it was processed for SDS-PAGE (Bio-Rad Criterion system). Each replicate was homogenized in an extraction buffer containing 50 mM Tris (pH 7.4), 2 mM EDTA, 5 mM EGTA, 0.1% SDS protease inhibitor cocktail type I (Roche) and II (Sigma). Homogenates were then centrifuged at 500 g at 4 °C and supernatants were collected. Protein concentration from each replicate supernatant was quantified using the Bradford protein assay (BioRad). Replicates were loaded at 30 μg and separated via electrophoresis in a 4–12% polyacrylamide gel, followed by sample preparation for proteomic analysis.

2.12. Label-free proteomics using 1D-SDS PAGE

1D Gels were divided into 6 sections using a Precision Plus Kaleidoscope standard (Bio-Rad) to indicate prominent proteins bands common to each lane as section boundaries. Gel sections were then excised and the resulting fractions were incubated in 200 mM Tris for 30 min followed by destaining with 50 mM Tris/50% acetonitrile for 1–2 h. Fractions were then dehydrated with 100% acetonitrile until gel pieces appeared opaque. Destaining was repeated a second time, followed by reduction with 20 mM DTT (Sigma) in 50 mM Tris for 1 h at 60 °C. Gel fraction dehydration and alkylation was done with 100% acetonitrile and 40 mM iodoacetamide (Sigma) in 50 mM Tris for 1 h at room temperature. Samples were rehydrated in 25 mM Tris and subjected to a final dehydration step prior to trypsin digest. Samples were mixed with 0.2–0.3 μg of trypsin (Promega) in 20 mM Tris/0.0002% zwittergent 3–16 overnight at 37 °C. Trypsin was inactivated and peptides were extracted by adding 2% trifluoroacetic acid to the digest for 30 min followed by the addition of acetonitrile for an additional 30 min. The supernatant was removed and saved, followed by addition of acetonitrile a third time to the gel fractions for 30 min. The gel fractions were then added to the saved supernatant. These peptide containing fractions were dried under vacuum and stored at −20 °C.

2.13. NanoLC tandem mass spectrometry (MS/MS)

Dried peptide extracts were reconstituted in an acidic aqueous solution of 0.2% formic, 0.1% TFA, and 0.001% zwittergent 3–16 detergent for analysis by nano-scale liquid chromatography interfaced to tandem mass spectrometry (nLC-MS/MS). Peptide mixture was loaded onto an Optipak 0.25 μl cartridge (Optimize Technologies, Oregon City, OR) custom packed with Michrom Magic C8 (Michrom BioResource, Auburn, CA) using an Eksigent nanoLC-Ultra 2D with AS3 autosampler. Peptides were separated by reverse-phase LC using a 75 μm i.d. fused silica column, packed in-house with 37 cm of 3um Magic C18 (Michrom BioResource) with a gradient of 2–40% B over 60 min with a mobile phase flow rate of 300 nL/min. Mobile phase A contained water, acetonitrile, and formic acid (98/2/0.2 by volume), whereas mobile phase B was composed of acetonitrile, isopropanol, water, and formic acid (80/10/10/0.2 by volume). Eluting peptides were analyzed using a Q-Exactive mass spectrometer (Thermo Fisher) configured to measure peptides within the molecular weight range of 360–2000 *m/z* at a resolving power of 70 K (FMHM, *m/z* 200) survey scans (MS1), followed by isolating top 15 most abundant ions for higher energy C-trap dissociation scans (MS2) using an isolation window of 2Da at a resolving power of 17.5 K and a 45 s exclusion duration [32].

2.14. Data processing and label-free quantification data analysis

Data files were imported into the Rosetta Elucidator software (Seattle, WA) in which a relatively quantitative label-free pipeline was used for analysis [33,34]. Features were detected such that *m/z*, retention time, and peak intensity alignment of MS1 data were extracted across samples. Database searching on features selected with charge state <4 and >1, peak confidence score >0.6, peak time score >0.8, and peak *m/z* score >0.9, was initiated within Elucidator using Mascot (v2.2, Matrix Science) with mouse Swiss-Prot database (release-2012_02) appended with common contaminants and a reverse decoy database. Mascot search parameters were set with peptide precursor tolerance of 10 ppm, ms/ms tolerance of 0.6Da, 2 missed cleavages, and variable modifications carbamidomethyl C, oxidation M, and propionamide C. Annotation was performed using the Peptide Prophet implementation in Elucidator. Detection of differentially expressed peak ratios was performed with ANOVA utilizing a signature *p* value decoy error rate of no more than 5%, and this annotation was assigned across aligned sample features so that relative quantitation of corresponding protein identifications across sample groups could be compared [35–37].

2.15. Heat map analysis and principal component analysis

Heat maps were drawn to determine the expression patterns of significantly up- or down-regulated protein at each time point and to compare the expression levels with the other time points, using R version 2.15.1 and the R packages. Principal component analysis (PCA) can reduce the dimensionality of a data set consisting of a large number of interrelated variables, while retaining as much as possible of the variation present in the data set. PCA was conducted as an "unsupervised" analysis to clarify the variance among microarray data from heart samples using R. To clarify the variances among samples, data were calculated using a Q-mode PCA package 'prcomp' of R. The proportion of variance and factor loading were also calculated.

2.16. Ingenuity pathway analysis

To classify the protein functionally, we used Ingenuity Pathway Analysis (IPA), where we entered the genes whose fold changes were more than 1.2-fold and P values were less than 0.05. IPA shows possible networks involved in microarray profiles by the IPA Network Generation Algorithm. Proteins were clustered and classified by the IPA Network Generation algorithm, and the network score ranked the networks. In the networks, solid and dashed lines indicated direct and indirect interactions, respectively. Direct interactions require the two molecules to make direct physical contact with each other; there is no intermediate step. Indirect interactions do not require physical contact between the two molecules, such as a signaling cascade, instead of the two molecules making physical contact with each other [[38].

2.17. Statistical analysis

All data are expressed as mean ± standard error of the mean (SEM). Statistics were performed using either a two-tailed Student's *t*-test (Prism, GraphPad Software, La Jolla, CA) or two-way measures ANOVA followed by a Tukey *post hoc* test (SigmaStat, SYSTAT software, Point Richmond, CA). The criterion for statistical significance was $p < 0.05$.

3. Results

3.1. Endothelial Ng expression is required for endothelial function in mice

To determine the in vivo role of Ng expression on endothelial function, Cre-CDH5-$Ng^{f/f}$ mice were generated using Cre-LoxP approaches. We then tested if the endothelial-specific knockout of Ng impairs endothelial and cardiac function using the FMD model and transthoracic echocardiography, respectively [25,26]. Endothelium-dependent dilatation of the femoral artery is contributed to by several factors, including NO activity and oxidative stress [28]. Using the FMD method, we

measured femoral artery diameter at baseline and for 5 min during reactive hyperemia after ischemia induced by an inflatable cuff near the lower limb. Endothelial-specific Ng knockout mice demonstrate a significant delay in the FMD response compared to control littermates (Fig. 1A), while there were no differences in heart rate, ejection fraction, fractional shortening, or cardiac output observed after echocardiography measurements in these mice (Fig. 1B). This result suggests that endothelial Ng expression is required for proper endothelial function but does not impact cardiac function.

3.2. Label-free proteomics analysis in the aorta of Cre-CDH5-Ng$^{f/f}$ mice

To further elucidate the function of endothelial Ng expression, proteomic analysis was performed on aortas from endothelial-specific Ng knockout mice and control littermates. Briefly, aorta tissues were isolated and lysed from four control and five Cre-CDH5-Ng$^{f/f}$ mice, and 1D-SDS PAGE separated each protein lysate. Protein quantification was processed using nanoLC-orbitrap-mass spectrometry (MS). Label-free quantification proteomics identified a total of 3837 proteins from the aorta of both control and Cre-CDH5-Ng$^{f/f}$ mice. To confirm MS data quality, MS peak intensity and its number from each aorta were analyzed using a density plot representing the distribution of variables (Fig. 1C). All the samples showed less than 10% variability in peptide number and peak intensity. We then profiled protein expression change between genotypes and generated a heat map for the significantly changed 656 proteins (Fig. 1D–Supplemental Table 1). To further determine whether Ng knockout in the endothelial cells alters protein expression patterns, we conducted PCA. Cre-CDH5-Ng$^{f/f}$ mice (red circle) showed significant differences according to principal component 1 (PC1) compared to wildtype mice (blue circle) (Fig. 1E). Depletion of Ng alters protein expressions that affect endothelial activation and nitric oxide production in the aorta, which is consistent with previous reports [26]. To gain more insight into the effects of Ng expression in the aorta, ingenuity pathway analysis (IPA) was conducted to map the biological processes regulated by endothelial-specific Ng knockout (Fig. 1F). IPA found that signaling networks related to mitochondrial dysfunction and redox biology abnormality (sirtuin, oxidative stress, and NRF2 mechanism) were significantly involved in the aortas of Cre-CDH5-Ng$^{f/f}$ mice. Then, IPA analysis suggested that cardiovascular disease and energy metabolism-related biological functions were significantly altered in the Cre-CDH5-Ng$^{f/f}$ mouse aortas as well. This approach revealed that a lack of Ng in endothelial cells may suppress ATP and NO production while enhancing Caveolin signaling in the vasculature (Fig. 1G). Finally, we selected 31 significant proteins from the aorta of Cre-CDH5-Ng$^{f/f}$ mice,

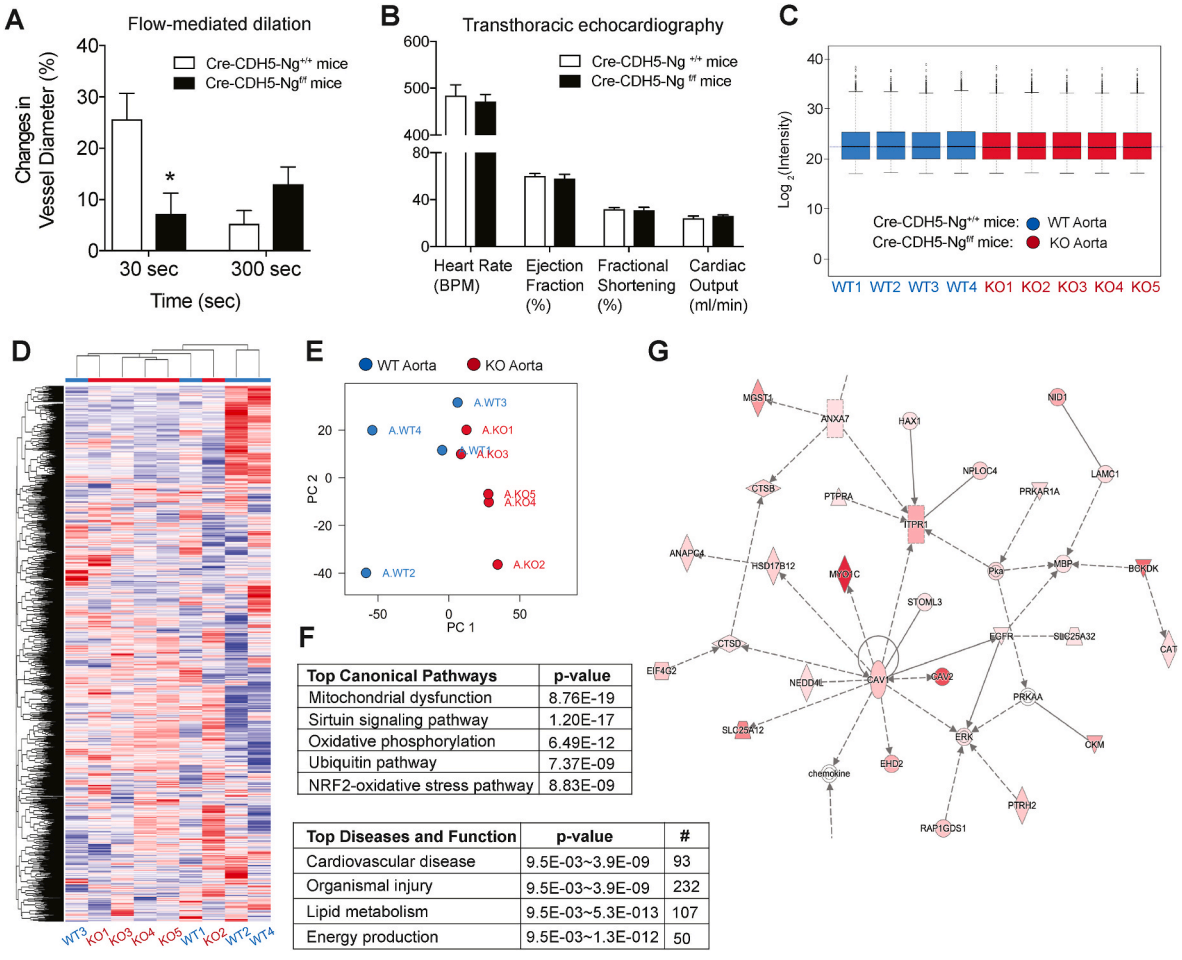

Top Canonical Pathways	p-value
Mitochondrial dysfunction	8.76E-19
Sirtuin signaling pathway	1.20E-17
Oxidative phosphorylation	6.49E-12
Ubiquitin pathway	7.37E-09
NRF2-oxidative stress pathway	8.83E-09

Top Diseases and Function	p-value	#
Cardiovascular disease	9.5E-03~3.9E-09	93
Organismal injury	9.5E-03~3.9E-09	232
Lipid metabolism	9.5E-03~5.3E-013	107
Energy production	9.5E-03~1.3E-012	50

Fig. 1. Ng regulates mitochondrial function in the endothelium of mice.
Fig. 1. **A.** Flow-mediated dilation performed in Cre-CDH5-Ng$^{+/+}$ and Cre-CDH5-Ng$^{f/f}$ mice suggests endothelial dysfunction occurs in mice lacking endothelial Ng expression. **B.** Transthoracic echocardiography results show no difference in heart rate, ejection fraction, fractional shortening, or cardiac output in mice. **C.** Density plot of MS peak intensity representing the distribution of variables in aorta samples. All samples indicated less than 10% of the variability in peptides number and peak intensity. **D.** Heat map for the 656 significantly changed proteins in the aorta samples. **E.** PCA of Cre-CDH5-Ng$^{f/f}$ mice (red circle) and wild-type mice (blue circle) showed significant differences according to principal component 1 (PC1). **F.** Ingenuity pathway analysis (IPA) results for the top canonical pathways and top diseases regulated by endothelial-specific Ng-knockout mice. **G.** Overall, this approach revealed that a lack of Ng in the endothelial cells may suppress ATP and NO production (n = 4–5/genotype).

indicating less than 0.05 p-value protein expression change (Table 1).

3.3. Neurogranin expression colocalizes with the mitochondria in endothelial cells

Since mitochondrial dysfunction is suggested to occur in the aortas of endothelial-specific Ng knockout mice, we sought to determine if Ng expression was associated with the mitochondria in HAECs. Subcellular fractionation assays and immunofluorescence experiments were employed to find the subcellular localization of Ng within endothelial cells. First, HAECs were biochemically fractionated into cytosolic, membrane, soluble nuclear, chromatin-bound nuclear, and cytoskeletal fractions. Then, cellular Ng expression in HAECs was detected using western blotting. We found that Ng protein is expressed in the cytosol, membrane, and soluble nuclear fractions, with no expression in the chromatin-bound or cytoskeleton fractions (Fig. 2A). The mitochondrial marker, COX IV, was dominantly expressed in the membrane and soluble nuclear fractions, like Ng. Ng's binding protein, CaM, was detected at low levels in the cytosolic fraction. However, immunofluorescence results indicate that Ng (red) colocalized with CaM (green) in the cytosolic area of HAECs (Fig. 2B). This finding indicates that Ng is expressed not only in the cytosol but also within other subcellular organelles, including mitochondria.

To further assess Ng expression in mitochondria, control, Ng knockdown (Ng siRNA), and Ng overexpression HAECs were separated using a mitochondria fractionation kit. Ng expression was seen in both cytosolic and mitochondrial fractions after western blotting. Strikingly, Ng expression levels seemed to be higher in the mitochondria fraction compared to other fractions, which has never been reported (Fig. 2C).

Table 1
Protein expression change in the aorta of Cre-CDH5 $Ng^{f/f}$ mice.

Gene Names	Protein Name	Ratio	p-value
Atp1b1	Sodium/potassium-transporting ATPase subunit	0.29	0.0001
Neb	Nebulin	0.26	0.0003
Myo1c	Myosin-Ic	1.69	0.0008
Ppp1r12a	Protein phosphatase 1 regulatory subunit	1.94	0.0012
Cav2	Caveolin-2	2.01	0.0015
Slc25a12	Calcium-binding mitochondrial carrier protein Aralar1	0.24	0.0038
Itpr1	Inositol 1,4,5-trisphosphate receptor type 1	1.38	0.0077
Ppp3ca	Serine/threonine-protein phosphatase 2B	0.52	0.0122
Pacsin3	Protein kinase C and casein kinase II substrate	0.28	0.0128
Cav1	Caveolin-1	1.54	0.0128
Apob	Apolipoprotein B-100	1.28	0.0132
Vwa8	von Willebrand factor A domain-containing protein 8	1.47	0.0207
Timm8a1	Mitochondrial import inner membrane translocase (Tim8 A)	1.64	0.0208
Prkar1a	cAMP-dependent protein kinase (alpha regulatory)	0.67	0.0220
Abcf1	ATP-binding cassette sub-family F member 1	1.33	0.0225
Gsk3b	Glycogen synthase kinase-3 beta	0.66	0.0234
Nos1	Nitric oxide synthase	0.56	0.0235
Atp5f1c	ATP synthase subunit gamma	0.65	0.0238
Cavin1	Caveolae-associated protein 1	1.30	0.0248
Cox7a2l	Cytochrome *c* oxidase subunit 7A	1.44	0.0291
Postn	Periostin	1.53	0.0291
Stoml3	Stomatin-like protein 3	1.66	0.0303
Cpt2	Carnitine O-palmitoyltransferase 2	1.32	0.0305
Timm22	Mitochondrial import inner membrane translocase (Tim22)	1.51	0.0312
Ppp3r1	Calcineurin subunit B	0.75	0.0325
Uqcrc2	Cytochrome *b-c*1 complex subunit 2	1.31	0.0380
Sh3glb1	Endophilin-B1	0.63	0.0411
Nckap1	Nck-associated protein 1	1.60	0.0414
Prkca	Protein kinase C alpha type	0.57	0.0415
Cavin4	Caveolae-associated protein 4	0.29	0.0419
Camk2d	Calcium/calmodulin-dependent protein kinase type II	0.68	0.0461

Immunofluorescence experiments also revealed Ng expression colocalized with the mitochondrial marker, cytochrome *c* oxidase IV (COX IV), in HAECs (Fig. 2D). Ng siRNA significantly decreases colocalization of Ng and COX IV. These results are the first to demonstrate that Ng protein expression is associated with the mitochondria in endothelial cells and may play a role in Ca^{2+}-dependent mitochondrial function and therefore, redox balance.

3.4. Ng expression positively impacts mitochondrial respiratory function

To elucidate the role of Ng expression on mitochondrial function, we measured the OCR of the electron transport chain using the Seahorse assay on control, scrambled control, siRNA-mediated Ng knockdown, and Ng overexpressed HAECs (Fig. 3A). No differences were seen in OCR between control and scrambled control groups. However, Ng knockdown (red bar) significantly decreased baseline OCR ($t = 4.08$, $df = 24$, $p < 0.001$) (Fig. 3B), maximal OCR after FCCP treatment ($t = 5.47$, $df = 24$, $p < 0.001$) (Fig. 3C), and ATP-linked OCR ($t = 3.53$, $df = 24$, $p < 0.01$) (Fig. 3D). Interestingly, overexpression of Ng (blue bar) significantly increased baseline ($t = 3.72$, $df = 24$, $p < 0.001$), maximal ($t = 4.66$, $df = 24$, $p < 0.0001$), and ATP-linked OCR in HAECs ($t = 5.02$, $df = 24$, $p < 0.0001$) (Fig. 3B–D). This finding indicates that Ng siRNA shows decreased mitochondrial OCR and ATP production, while Ng overexpression shows increased mitochondrial OCR and ATP production.

3.5. MitoEbselen treatment rescues baseline OCR in Ng knockdown HAECs

Chronic, sustained increases in H_2O_2 can negatively impact mitochondrial functioning and OCR [39]. MitoEbselen is a GPx mimetic that scavenges mitochondrial-specific H_2O_2 [40]. MitoEbselen demonstrates potent antioxidant activity and has been observed to preserve cell function during oxidative stress in many cell types and disease models, including cardiovascular disease [41]. Furthermore, H_2O_2 scavenging by MitoEbselen has been seen to positively influence OCR and mitochondrial function in multiple cell types, including endothelial cells [42,43].

Therefore, we wanted to know if the altered OCR changes observed in response to Ng expression level were due to increased mtROS production. To evaluate this, cells were pretreated with MitoEbselen (1 nM) 30 min before OCR measurement in control, Ng siRNA, and Ng overexpression conditions. Two-way ANOVA showed that MitoEbselen treatment in control cells significantly increases OCR in MitoEbselen treatment [$F(1,216) = 1475$, $p < 0.001$)], mitochondrial respiration change by Oligomycin, FCCP, and Rotenone/Antimycin A [$F(11,216) = 223.7$, $p < 0.001$)], and interactions [$F(11,216) = 91.92$, $p < 0.001$)] (Fig. 3E). MitoEbselen treatment in Ng siRNA rescued the decreased baseline and maximum OCR seen in Ng knockdown pHAECs to control levels. Two-way ANOVA indicated that MitoEbselen treatment in Ng siRNA significantly increases OCR in MitoEbselen treatment [$F(1,144) = 50.28$, $p < 0.001$)], mitochondrial respiration change by Oligomycin, FCCP, and Rotenone/Antimycin A [$F(11,144) = 6.54$, $p < 0.001$)], without interactions (Fig. 3F). Finally, although Ng overexpression in HAECs demonstrated significantly increased baseline OCR compared to control and Ng siRNA, Two-way ANOVA identified that MitoEbselen treatment in Ng overexpression did not impact OCR change (Fig. 3G). This finding indicates that while MitoEbselen treatment increases OCR in Ng knockdown cells, it does not further increase mitochondrial function in Ng overexpression cells due to a ceiling effect.

We then wanted to further determine the effect of MitoEbselen treatment on OCR by Ng expression levels in HAECs. Individual student t-tests found that MitoEbselen treatment significantly increases baseline OCR in control ($t = 11.6$, $df = 18$, $p < 0.001$) and Ng siRNA ($t = 2.4$, $df = 12$, $p < 0.05$), but had no effect on Ng overexpression HAECs (Fig. 3H). MitoEbselen treatment also increases maximum OCR (FCCP)

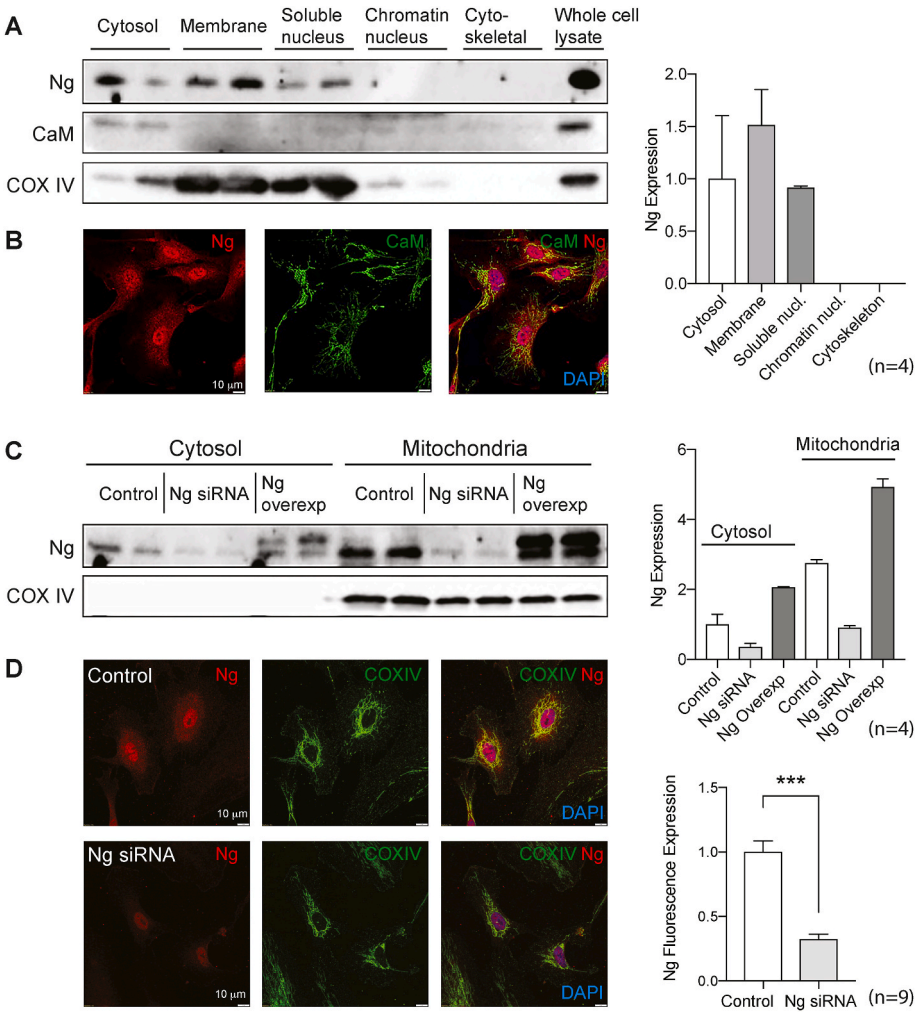

Fig. 2. Ng expression colocalizes with mitochondria in HAECs.
A. Western blot analysis of HAECs separated into cytosolic, membrane, soluble nuclear, chromatin-bound nuclear, and cytoskeletal fractions. Ng and COX IV expressions are seen in the cytosolic, membrane, and soluble nuclear fractions (n = 4). **B.** Immunofluorescence staining showing Ng (red) expression colocalized with CaM (green) in endothelial cells. **C.** Western blot of HAECs separated into cytosolic and mitochondrial fractions under control, Ng siRNA, and Ng overexpression conditions. Ng expression is seen in both fractions, with higher expression in the mitochondrial fraction (n = 4). **D.** Immunofluorescence staining of Ng in control and Ng siRNA endothelial cells. Ng protein (red) colocalizes with the mitochondrial marker, COX IV protein (green) (n = 9).

in control ($t = 17.8$, $df = 18$, $p < 0.0001$) and Ng siRNA ($t = 2.2$, $df = 12$, $p < 0.05$). But had no effect on Ng overexpression HAECs (Fig. 3I). These results may indicate that Ng overexpression maximizes mitochondrial function, which cannot be further influenced by MitoEbselen. In addition, MitoEbselen treatment had no effect on ATP production in both Ng siRNA and overexpression conditions, while it showed increased ATP production in control HAECs ($t = 13.8$, $df = 18$, $p < 0.0001$) (Fig. 3J). In Ng siRNA, MitoEbselen treatment rescued decreased OCR, but had no effect on ATP production. In Ng overexpression cells, MitoEbselen treatment showed no effect on OCR and ATP production. Overall, these findings indicated that mitochondrial Ng expression plays a distinct role between ATP production (Complex V) and H_2O_2 generation throughout different mechanisms.

3.6. *Ng knockdown increases mitochondrial-H_2O_2 production in endothelial cells*

MitoEbselen, which neutralizes mitochondrial-specific H_2O_2, significantly rescued the decreased mitochondrial respiration in Ng knockdown cells during the Seahorse assay. Therefore, we wanted to further assess H_2O_2 levels in these cells. In order to measure mitochondrial-specific H_2O_2 levels, a Telo-HAEC cell line expressing a mitochondria-targeted roGFP2-Orp1 (mito-Orp1) H_2O_2 sensor was used that involves a redox-sensitive roGFP2 fused with the yeast thiol peroxidase ORP1 [44–46]. H_2O_2 can react with the thiol of ORP1 to ultimately cause a reversible thiol-disulfide exchange between the chromophores, which increases the 395 nm excitation peak of Orp1 and decreases the 480 nm excitation peak of roGFP2, thereby increasing the 395/480 nm ratio (Fig. 4A). Images were taken of control, Ng knockdown, and Ng overexpression cells expressing mito-Orp1 under untreated, MitoEbselen pretreatment, fully reduced (DTT-treated), and fully oxidized (DMD-treated) conditions for 20 min and ratios analyzed using NIS elements software (Supplemental Fig. 1). Ng knockdown cells had a significantly higher normalized 395/480 ratio than control cells throughout the 20 min (Fig. 4C, $p < 0.005$) and when averaged (Fig. 4D, $p < 0.005$), indicating higher mitochondrial H_2O_2 levels. Surprisingly, cells overexpressing Ng also had a significantly higher ratio than the control ($p < 0.05$). After pretreatment with MitoEbselen, H_2O_2 levels were decreased across all conditions. Consequently, MitoEbselen treatment stabilized the mitochondrial H_2O_2 imbalance induced by Ng siRNA and Ng overexpression in HAECs, implicating its role as a therapeutic approach to alleviate redox imbalance. In addition, we also measured $O_2^{\bullet-}$ levels in HAECs under control, Ng siRNA, and Ng overexpression conditions (Fig. 4E). Ng knockdown and Ng overexpression did not

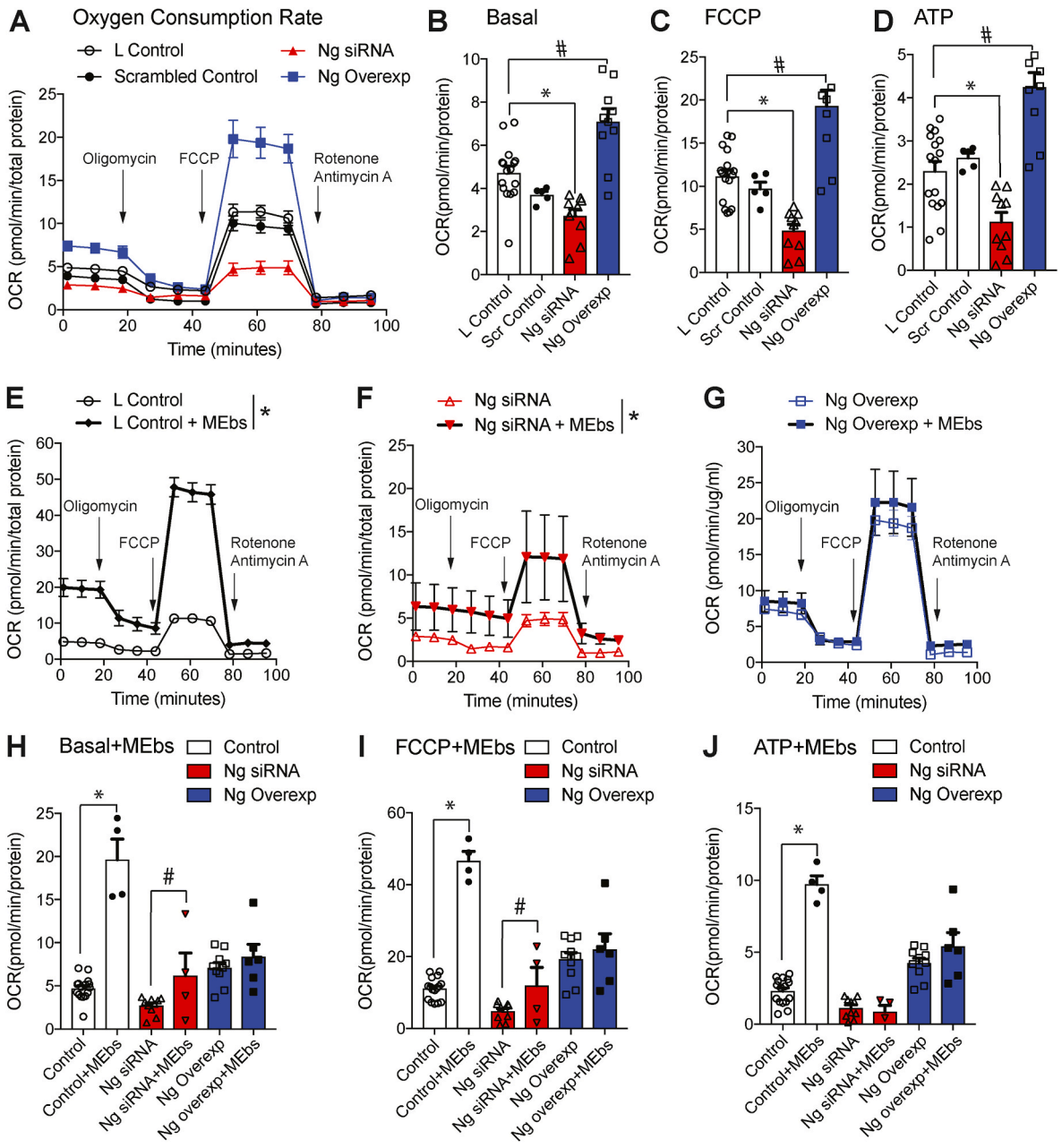

Fig. 3. Decreased Ng expression decreases mitochondrial function in HAECs.
A. Seahorse assay profiles of oxygen consumption rate (OCR) in Lipofectamine control (L control), Scrambled control, Ng knockdown (Ng siRNA), and Ng overexpression (Ng Overexp) in HAECs. Decreased Ng expression in HAECs significantly decreased OCR at **B.** baseline, **C.** maximum capacity, and **D.** ATP turnover, whereas overexpression of Ng significantly increased OCR at baseline, maximum capacity, and ATP turnover (n = 5–10, *p < 0.001, #p < 0.001). Seahorse assay profiles of control treatment and MitoEbselen (MEbs)-treated HAECs under **E.** L control, **F.** Ng siRNA, and **G.** Ng Overexp conditions. For the treatment group, cells were treated with 1 nM MEbs for 30 min prior to Seahorse measurements. MEbs treatment rescues decreased **H.** baseline and **I.** maximum OCR, but not **J.** ATP turnover in Ng knockdown HAECs. No effect was seen on Ng overexpression cells after MEbs treatment. (n = 4–10, *, #p < 0.001 between treatments).

significantly alter $O_2^{\bullet-}$ levels, while MitoEbselen treatment decreases $O_2^{\bullet-}$ in control. These results suggest that Ng expression plays an essential role in mitochondrial-H_2O_2 balance.

3.7. *MitoEbselen rescues decreased eNOS expression and NO levels in Ng knockdown HAECs*

In this study, we found that MitoEbselen treatment increases OCR and decreases mitochondrial-H_2O_2 levels in Ng knockdown HAECs. It is reported that a lack of cytosolic Ng expression has been seen to decrease eNOS activity and NO bioavailability in HAECs, which plays an important role in endothelial activation and the pathophysiology of vascular diseases [26]. Therefore, it is important to evaluate the causal relationship between Ng-mediated mtROS production and eNOS regulation. We hypothesize that Ng-mediated mtROS production affects eNOS expression/function and NO bioavailability. To test this hypothesis, we assessed the impact of MitoEbselen treatment on eNOS expression and function in HAECs under control, Ng knockdown, and Ng overexpression conditions. To evaluate eNOS expression, western blotting was performed on whole cell lysates from untreated and MitoEbselen-pretreated mock, Ng siRNA, and Ng overexpression HAECs (Fig. 5A). Ng expression was seen to significantly increase after MitoEbselen treatment in all groups (Fig. 5B). eNOS expression was significantly decreased in Ng siRNA cells compared to mock control.

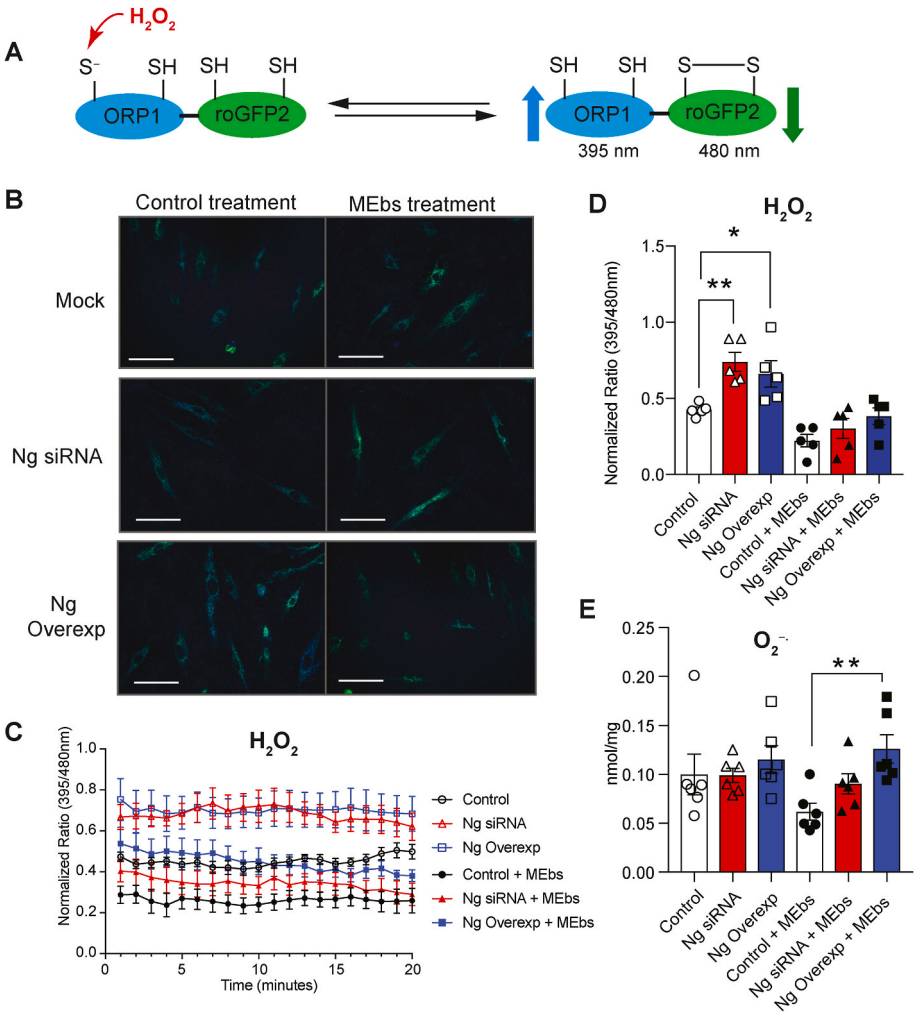

Fig. 4. Ng knockdown increases mitochondrial-hydrogen peroxide production in endothelial cells.
A. Schematic of the roGFP2-Orp1 probe responding reversibly to changes in H_2O_2 [44]. **B.** Fluorescent images of the mito-roGFP2-Orp1 probe in control, Ng siRNA, and Ng overexpression Telo-HAECs (20X). **C.** Fluorescence ratios (395/480 nm, normalized to the highest value) of Mito-roGFP2-Orp1 detected over time. **D.** Averaged normalized fluorescence ratios of Mito-roGFP2-Orp1 indicate that Ng knockdown and overexpression increase mitochondrial H_2O_2 production. Cells treated with 1 nM MEbs for 30 min before imaging demonstrate decreased H_2O_2 levels. ($n = 5$, $^*p < 0.05$, $^{**}p < 0.005$). **E.** Ng knockdown and Ng overexpression did not significantly alter $O_2^{\bullet-}$ levels, while MitoEbselen treatment decreases $O_2^{\bullet-}$ in control cells. For the MEbs treatment group, cells were incubated with 1 nM MEbs for 30 min before samples were prepared for HPLC analysis ($n = 6$, $^*p < 0.05$, $^{**}p < 0.005$).

Strikingly, this was rescued in the siRNA after the addition of MitoEbselen (Fig. 5C). Overexpression of Ng slightly decreased eNOS expression in HAECs. MitoEbselen rescued it, but there was no statistical significance. There was no change in eNOS phosphorylation at its activation site (S1177) in Ng siRNA, while overexpression showed an increased phospho-eNOS. However, the MitoEbselen treatment did not change eNOS phosphorylation in mock, Ng siRNA, and Ng overexpression (Fig. 5D).

Finally, NO cellular levels were measured using a Sievers Nitric Oxide Analyzer 280i [31]. Ng siRNA cells had significantly lower NO levels compared to the control. This was rescued to control levels after the treatment of MitoEbselen (Fig. 5E). Ng overexpression did not alter NO levels compared to control levels even after MitoEbselen treatment. This finding implies that decreased Ng expression is important in NO dysfunction in HAECs. Moreover, decreased Ng expression in the mitochondria increases H_2O_2 production, which may impact eNOS expression, leading to redox imbalance with decreased NO and endothelial dysfunction.

4. Discussion

In this study, we are the first to detect Ng expression colocalized with the mitochondria in endothelial cells and how alterations of Ng expression affect mitochondrial function and redox balance. Proteomic analysis of aortas from endothelial-specific Ng knockout mice suggests mitochondrial dysfunction as the top canonical pathway altered in these mice compared to control animals. This proteomics approach allowed us to investigate the role of Ng expression within the mitochondria in endothelial cells. We chose to perform subcellular fractionation assays in order to probe for Ng protein expression in distinct cellular compartments with Western blot. Interestingly, expression of the inner mitochondrial membrane marker, COX IV, was detected in the same fractions as Ng with the first assay used. We also identified Ng expression in the cytosolic and mitochondrial fractions of HAECs using a second assay, with Ng expression being higher in the mitochondrial fraction. This evidence is the first to suggest a role for Ng associated with the mitochondria in endothelial cells.

Previously, global Ng knockout ($Ng^{-/-}$) mice demonstrated cardiac hypertrophy, heart failure, and endothelial dysfunction [25,26]. In this study, we generated Cre-CDH5-$Ng^{f/f}$ and assessed their cardiovascular

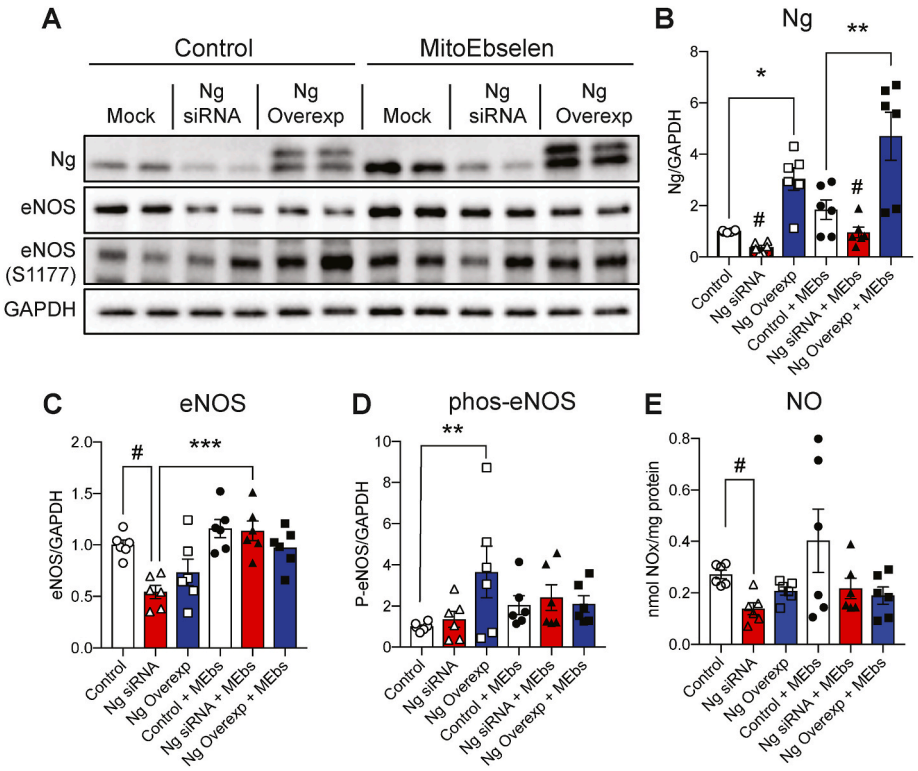

Fig. 5. MitoEbselen treatment rescues eNOS expression and NO levels in Ng knockdown cells.
A. Western blot analysis of HAECs under control, Ng siRNA, and Ng overexpression conditions. Cells were either left untreated or incubated with 1 nM MEbs for 30 min before cell lysis. **B.** MEbs treatment increases Ng expression in HAECs ($n = 6$, $^{*}p < 0.05$, $^{**}p < 0.005$, $\#p < 0.05$ between control and Ng siRNA). **C.** Ng siRNA showed decreased eNOS expression in HAECs. MEbs treatment rescues decreased eNOS expression in Ng knockdown cells ($n = 6$, $^{***}p < 0.0005$, $\#p < 0.05$ between control and Ng siRNA). **D.** Ng overexpression significantly increases phospho-eNOS (S1177) expression, which is decreased by MEbs treatment ($n = 6$, $^{**}p < 0.005$). **E.** Ng siRNA shows decreased NO levels. 30 min 1 nM MEbs treatment increases NO levels in control, and rescues decreased NO levels in Ng siRNA HAECs ($n = 6$, $\#p < 0.05$ between control and Ng siRNA).

phenotype. Transthoracic echocardiography showed no genotype differences in heart rate, ejection fraction, fractional shortening, or cardiac output. Interestingly, Cre-CDH5-Ng$^{f/f}$ mice display defective endothelial function measured by FMD, consistent with the Ng$^{-/-}$mouse phenotype. These results strongly suggest that endothelial Ng expression is essential in sustaining endothelial homeostasis.

Using label-free proteomics, we analyzed the proteome change in the aortas from Cre-CDH5-Ng$^{f/f}$ compared to Ng$^{f/f}$ mice. Recent advances in proteomics methodologies serve as powerful platforms for generating hypotheses and discovering underlying mechanisms. Label-free proteomics is a technique used to quantify and compare proteins in complex biological samples without needing stable isotopic labeling or synthetic peptides [32,34,47]. Although it limits sample complexity, dynamics range, and quantification accuracy due to the simultaneous analysis of numerous proteins, our experimental design using Cre-CDH5-Ng$^{f/f}$ mice, rigorous sample preparation, optimized instrumentation of Orbitrap fusion mass spectrometry, and robust data analysis strategies can help maximize the benefits. Overall, our IPA analysis identifies novel mtROS and NO pathways relevant to cardiovascular disease and mitochondria metabolism changes in the aorta of Cre-CDH5-Ng$^{f/f}$ mice. Genetic variants of Ng are significantly observed in neurological disease populations, including Alzheimer's disease and schizophrenia [48,49]. Although Ng expression is known to affect Ca^{2+}-dependent excitotoxicity in the neuron, the mechanism of how Ng contributes to the pathophysiology of brain diseases remains unclear. In addition, the role of Ng expression in skeletal muscle, endothelial cells, and cardiomyocytes has been studied recently, but its relevance in human disease has yet been studied. Therefore, our proteomics study exploring the role of Ng expression on mitochondrial respiration and mtROS production is important for expanding the information on the Ng mechanism in redox biology and human brain and vascular diseases.

Most previous studies suggest that Ng expression is associated with the cytosol and plasma membrane in neurons [50–52]. Interestingly, Ng immunolabeling associated with the outer mitochondrial membrane (OMM) has been observed in pyramidal neurons with electron microscopy (EM) [27]. However, the role of Ng expression in the mitochondria has never been studied. In this study, Ng expression was seen colocalized with the mitochondrial marker (COX IV) in HAECs with subcellular fractionation, Western blot, and immunofluorescence. However, we still do not know if Ng is associated with the inner mitochondrial membrane or matrix in endothelial cells. Even though there is no mitochondrial targeting sequence in Ng, depletion of Ng decreases OCR and ATP production while it increases H_2O_2. Thus, we anticipate that Ng is also expressed in multiple mitochondrial compartments since oxidative phosphorylation and ATP synthesis occur in the inner mitochondrial membrane. At the same time, the matrix is particularly sensitive to calcium regulation. To determine Ng expression in mitochondria compartments, biochemical mitochondrial fractionation using a density gradient and EM experiments are needed in the future. In addition, to validate the functional significance of Ng expression in mitochondria compartments, the effects of mitochondria-targeted Ng overexpression or re-expression of mitochondria-targeted Ng in aortic endothelial cells isolated from Cre-CD5-Ng$^{f/f}$ mice should be examined. Previous studies have suggested activity-dependent translocation of Ng to the nucleus in neurons [53]. We also observed Ng expression in the soluble nuclear fraction and immunofluorescence staining of the HAECs. These results imply that Ng may have additional functions associated with the nucleus in endothelial cells, which requires further studies. Overall, Ng regulation in endothelial cells is still new, and the subcellular function of Ng in endothelial cells has never been reported. Thus,

we chose to focus on the role of Ng expression on mitochondrial function and redox balance.

$O_2^{\bullet-}$ is generated by complexes I and III of the electron transport chain, and chronically elevated levels of mtROS can induce mitochondrial dysfunction and subsequent endothelial dysfunction [3–5,10]. We found that mitochondrial Ng expression change did not impact $O_2^{\bullet-}$ (Fig. 4E). However, alteration of Ng expression, including Ng siRNA and Ng overexpression, increases H_2O_2 levels (Fig. 4D). This finding may indicate that Ng expression is not related to mitochondrial electron transfer process through complexes I and III, which is critical for $O_2^{\bullet-}$ generation. However, our results demonstrate that Ng expression is a crucial regulator of mitochondrial OCR, ATP, and H_2O_2 production in endothelial cells. Ng siRNA in HAECs significantly decreased mitochondrial function via OCR through decreased baseline, maximum OCR, and ATP turnover, while Ng overexpression increased mitochondrial function observed in the Seahorse assay (Fig. 3A). These findings implicate that Ng expression also regulates ATP synthase (complex V). Since we observed a decreased ATP synthase expression in our proteomic finding from Cre-CDH5-Ng f/f mice (Table 1), decreased ATP in the Ng siRNA is the anticipated outcome.

Oligomycin inhibits mitochondrial ATP synthase (complex V). During the Seahorse assay, non-ATP–linked OCR is equal to the rate observed in the presence of oligomycin. Thus, ATP-linked OCR can be calculated by subtracting non-ATP-linked OCR from the baseline OCR. Our Seahorse assay experiments revealed that Ng knockdown in HAECs significantly decreased ATP-linked OCR, while Ng overexpression significantly increased ATP-linked OCR. Antioxidant MitoEbselen treatment significantly increased ATP turnover in control HAECs but did not affect ATP-linked OCR under Ng knockdown or overexpression conditions. This was interesting to observe as MitoEbselen treatment was seen to decrease mitochondrial H_2O_2 levels in Ng knockdown and overexpression HAECs to those lower than control levels. Therefore, this data further implies that Ng expression may play a direct role in complex V of the electron transport chain in HAECs, independent of mtROS production, which should be studied further.

$O_2^{\bullet-}$ produced by the electron transport chain is promptly converted into H_2O_2 by mitochondrial superoxide dismutase (MnSOD) and then to O_2 and H_2O by GPx or catalase [10]. In this study, we wanted to explore the role of Ng on mtROS production, specifically H_2O_2, in endothelial cells. For this experiment, we chose to use the mito-Orp1 probe because this is the only current method to measure mitochondrial-specific H_2O_2 [44]. Other methods, such as HyPer are pH-sensitive, or in the case of Amplex Red, measure whole-cell H_2O_2, are less specific. Our Mito-Orp1 experiments revealed that altering Ng expression significantly increases mtROS production. H_2O_2 levels in both Ng knockdown and Ng overexpression HAECs were significantly increased, with Ng knockdown showing a more dramatic increase. $O_2^{\bullet-}$ levels were also measured in these cells but were not altered across conditions. This data suggests that since altered Ng expression increases mitochondrial H_2O_2 levels but not $O_2^{\bullet-}$, there may be a disruption in MnSOD or GPx antioxidant system when Ng expression is affected. Therefore, future studies are required to elucidate the effects of Ng expression on antioxidant signaling within CVD.

Decreased NO availability can occur due to increased production of mtROS and mitochondrial dysfunction [3–5]. However, it is not clear whether this decrease in NO is more dependent on the uncoupling and inactivation of eNOS or the direct actions of mtROS on NO. In this study, we demonstrated that Ng knockdown in HAECs causes mitochondrial dysfunction and increases mtROS production, which consequently decreases eNOS expression and NO levels. Mitochondrial-specific MitoEbselen treatment was seen to rescue the decreased eNOS expression and NO levels in Ng knockdown HAECs to control levels, which suggests that Ng-mediated mtROS production plays an important role in NO availability. Under Ng siRNA conditions, MitoEbselen treatment significantly increased OCR and NO levels in HAECs. However, eNOS expression was only moderately increased in control cells. Together, this suggests that NO availability observed in HAECs is predominantly regulated by Ng-mediated mtROS production compared to Ng-mediated eNOS expression.

MitoEbselen demonstrates potent antioxidant activity and has been observed to preserve cell function during oxidative stress in many cell types and disease models, including cardiovascular disease [41]. Chronic, sustained increases in H_2O_2 can negatively impact mitochondrial functioning and OCR. Therefore, H_2O_2 scavenging by MitoEbselen has been seen to positively influence OCR and mitochondrial function in multiple cell types, including endothelial cells [42,43]. Notably, MitoEbselen treatment does not further increase OCR in Ng overexpression HAECs, which hints that a different pathway may become dominant in endothelial cells when Ng is overexpressed. Also, Ng overexpression HAECs did not display significantly altered eNOS expression or NO levels compared to control and were not affected by MitoEbselen either. However, these cells did have significantly increased phospho-eNOS (S1177) expression, which was decreased with MitoEbselen treatment. Mostly, the depletion of Ng demonstrates adverse clinical outcomes in humans [48,49,54–57], while Ng overexpression has been shown to play a protective role [58,59]. Therefore, we employed Ng overexpression as a rescue control of Ng siRNA, but we found that Ng overexpression also has a detrimental effect on H_2O_2 production in HAECs. This further implies the upregulation of another molecular pathway, possibly CaMKII, when Ng is overexpressed in endothelial cells [60,61].

Previous studies have demonstrated that eNOS expression is decreased in response to the addition of H_2O_2 through AP-1 activity in endothelial cells [62]. Mitochondrial-derived H_2O_2 is known to depolarize mitochondrial membrane potential, limit mitochondrial Ca^{2+} uptake, and thereby decrease activity of the electron transport chain in endothelial cells [63]. Consistently, we observed that both Ng knockout and Ng overexpression significantly increase H_2O_2 production and affect eNOS expression. While slightly decreased eNOS expression was observed in Ng overexpression HAECs, this was insignificant and highly variable. In addition, overexpression of Ng does increase mitochondrial function. Several studies have implicated CaMKII in mediating membrane potential and mitochondrial function [64,65]. This could indicate a role for Ng-mediated Ca^{2+}-CaM-dependent signaling on mitochondrial function. Therefore, future studies should be conducted to test if altering mitochondrial Ng expression affects downstream Ca^{2+}-CaM-dependent signaling. This will help further elucidate the mechanism of Ng-mediated OCR and eNOS activation in these cells.

Overall, we have shown that mitochondrial Ng expression is crucial for mitochondrial function and regulating mtROS production in endothelial cells, while cytosolic Ng expression is required for eNOS expression and NO production. Dysfunctions in Ng expression increase mtROS production, which can cause mitochondrial dysfunction, decreased eNOS expression and NO availability, which can ultimately lead to endothelial dysfunction in cardiovascular disease. This data reveals the critical role of Ng in mtROS-NO balance in the endothelial cells, which should be studied further.

Sources of funding

This work was supported by an Institutional Development Award from the National Institutes of General Medical Sciences of the National Institutes of Health (NIH) under grant number P20GM121307 to C.G. Kevil, HL 139755 to C.B. Pattillo, and the NARSAD Young Investigator Award (26530) from the Brain & Behavior Research Foundation to H.W. Nam.

CRediT authorship contribution statement

Ashton N. Jorgensen: Writing – review & editing, Writing – original draft, Methodology, Investigation, Formal analysis, Conceptualization. **Nabil A. Rashdan:** Methodology, Investigation, Formal analysis, Data

curation. **K.N. Shashanka Rao:** Methodology, Investigation, Formal analysis, Data curation. **Luisa F. Delgadillo:** Methodology, Investigation, Formal analysis, Data curation. **Gopi K. Kolluru:** Methodology, Investigation, Formal analysis, Data curation. **David M. Krzywanski:** Supervision, Project administration, Funding acquisition. **Christopher B. Pattillo:** Supervision, Project administration, Funding acquisition. **Christopher G. Kevil:** Supervision, Project administration, Funding acquisition. **Hyung W. Nam:** Writing – review & editing, Writing – original draft, Visualization, Supervision, Software, Resources, Project administration, Methodology, Investigation, Funding acquisition, Conceptualization.

Declaration of competing interest

Declarations of interest: none.

Data availability

Data will be made available on request.

Acknowledgments

IDeA National Resource conducted label-free proteomics and the bioinformatic experiment for Quantitative Proteomics at the University of Arkansas for Medical Sciences. We thank Dr. Rona Scott for the support of the IPA analysis of this manuscript and the COBRE bioinformatics core for technical support.

Appendix A. Supplementary data

Supplementary data to this article can be found online at https://doi.org/10.1016/j.redox.2024.103085.

References

[1] J. Bailey, et al., A novel role for endothelial tetrahydrobiopterin in mitochondrial redox balance, Free Radic. Biol. Med. 104 (2017) 214–225.
[2] M.E. Widlansky, et al., The clinical implications of endothelial dysfunction, J. Am. Coll. Cardiol. 42 (7) (2003) 1149–1160.
[3] H. Cai, D.G. Harrison, Endothelial dysfunction in cardiovascular diseases: the role of oxidant stress, Circ. Res. 87 (10) (2000) 840–844.
[4] E. Galkina, K. Ley, Immune and inflammatory mechanisms of atherosclerosis (*), Annu. Rev. Immunol. 27 (2009) 165–197.
[5] K.N.S. Rao, et al., Nicotinamide nucleotide transhydrogenase (NNT) regulates mitochondrial ROS and endothelial dysfunction in response to angiotensin II, Redox Biol. 36 (2020) 101650.
[6] A. Szewczyk, et al., Mitochondrial mechanisms of endothelial dysfunction, Pharmacol. Rep. 67 (4) (2015) 704–710.
[7] M.A. Kluge, J.L. Fetterman, J.A. Vita, Mitochondria and endothelial function, Circ. Res. 112 (8) (2013) 1171–1188.
[8] V. Darley-Usmar, The powerhouse takes control of the cell; the role of mitochondria in signal transduction, Free Radic. Biol. Med. 37 (6) (2004) 753–754.
[9] M.E. Widlansky, D.D. Gutterman, Regulation of endothelial function by mitochondrial reactive oxygen species, Antioxid Redox Signal 15 (6) (2011) 1517–1530.
[10] M.D. Brand, et al., Mitochondrial superoxide: production, biological effects, and activation of uncoupling proteins, Free Radic. Biol. Med. 37 (6) (2004) 755–767.
[11] A. Gorlach, et al., Calcium and ROS: a mutual interplay, Redox Biol. 6 (2015) 260–271.
[12] A.M. Zafari, et al., Role of NADH/NADPH oxidase-derived H2O2 in angiotensin II-induced vascular hypertrophy, Hypertension 32 (3) (1998) 488–495.
[13] B.R. Silva, L. Pernomian, L.M. Bendhack, Contribution of oxidative stress to endothelial dysfunction in hypertension, Front. Physiol. 3 (2012) 441.
[14] N.R. Madamanchi, M.S. Runge, Mitochondrial dysfunction in atherosclerosis, Circ. Res. 100 (4) (2007) 460–473.
[15] A.J. Case, J. Tian, M.C. Zimmerman, Increased mitochondrial superoxide in the brain, but not periphery, sensitizes mice to angiotensin II-mediated hypertension, Redox Biol. 11 (2017) 82–90.
[16] T.J. Costa, et al., The homeostatic role of hydrogen peroxide, superoxide anion and nitric oxide in the vasculature, Free Radic. Biol. Med. 162 (2021) 615–635.
[17] E. Bertero, C. Maack, Calcium signaling and reactive oxygen species in mitochondria, Circ. Res. 122 (10) (2018) 1460–1478.
[18] C.W. Mahoney, J.H. Pak, K.P. Huang, Nitric oxide modification of rat brain neurogranin. Identification of the cysteine residues involved in intramolecular disulfide bridge formation using site-directed mutagenesis, J. Biol. Chem. 271 (46) (1996) 28798–28804.
[19] H.H. Miao, et al., Oxidative modification of neurogranin by nitric oxide: an amperometric study, Bioelectrochemistry 51 (2) (2000) 163–173.
[20] L.A. Jurado, P.S. Chockalingam, H.W. Jarrett, Apocalmodulin. Physiol Rev 79 (3) (1999) 661–682.
[21] A. Houdusse, et al., Crystal structure of apo-calmodulin bound to the first two IQ motifs of myosin V reveals essential recognition features, Proc. Natl. Acad. Sci. U. S. A. 103 (51) (2006) 19326–19331.
[22] T. Miyakawa, et al., Hyperactivity and intact hippocampus-dependent learning in mice lacking the M1 muscarinic acetylcholine receptor, J. Neurosci. 21 (14) (2001) 5239–5250.
[23] A.A. Nielsen, et al., Activation of the brain-specific neurogranin gene in murine T-cell lymphomas by proviral insertional mutagenesis, Gene 442 (1–2) (2009) 55–62.
[24] V.A. Fajardo, et al., Neurogranin is expressed in mammalian skeletal muscle and inhibits calcineurin signaling and myoblast fusion, Am. J. Physiol. Cell Physiol. 317 (5) (2019) C1025–C1033.
[25] A.N. Jorgensen, et al., Neurogranin regulates calcium-dependent cardiac hypertrophy, Exp. Mol. Pathol. 127 (2022) 104815.
[26] V.T. Cheriyan, et al., Neurogranin regulates eNOS function and endothelial activation, Redox Biol. (2020) 101487.
[27] M. Neuner-Jehle, J.P. Denizot, J. Mallet, Neurogranin is locally concentrated in rat cortical and hippocampal neurons, Brain Res. 733 (1) (1996) 149–154.
[28] D. Schuler, et al., Measurement of endothelium-dependent vasodilation in mice–brief report, Arterioscler. Thromb. Vasc. Biol. 34 (12) (2014) 2651–2657.
[29] R.B. Hinton Jr., et al., Mouse heart valve structure and function: echocardiographic and morphometric analyses from the fetus through the aged adult, Am. J. Physiol. Heart Circ. Physiol. 294 (6) (2008) H2480–H2488.
[30] J. Zielonka, J. Vasquez-Vivar, B. Kalyanaraman, Detection of 2-hydroxyethidium in cellular systems: a unique marker product of superoxide and hydroethidine, Nat. Protoc. 3 (1) (2008) 8–21.
[31] G.K. Kolluru, et al., H2S regulation of nitric oxide metabolism, Methods Enzymol. 554 (2015) 271–297.
[32] J.R. Ayers-Ringler, et al., Label-free proteomic analysis of protein changes in the striatum during chronic ethanol use and early withdrawal, Front. Behav. Neurosci. 10 (2016) 46.
[33] H. Neubert, et al., Label-free detection of differential protein expression by LC/MALDI mass spectrometry, J. Proteome Res. 7 (6) (2008) 2270–2279.
[34] M.C. Wiener, et al., Differential mass spectrometry: a label-free LC-MS method for finding significant differences in complex peptide and protein mixtures, Anal. Chem. 76 (20) (2004) 6085–6096.
[35] J.E. Elias, S.P. Gygi, Target-decoy search strategy for increased confidence in large-scale protein identifications by mass spectrometry, Nat. Methods 4 (3) (2007) 207–214.
[36] B.O. Keller, Z. Wang, L. Li, Low-mass proteome analysis based on liquid chromatography fractionation, nanoliter protein concentration/digestion, and microspot matrix-assisted laser desorption ionization mass spectrometry, J. Chromatogr., B: Anal. Technol. Biomed. Life Sci. 782 (1–2) (2002) 317–329.
[37] A.I. Nesvizhskii, et al., A statistical model for identifying proteins by tandem mass spectrometry, Anal. Chem. 75 (17) (2003) 4646–4658.
[38] S. Omura, et al., Bioinformatics multivariate analysis determined a set of phase-specific biomarker candidates in a novel mouse model for viral myocarditis, Circ Cardiovasc Genet 7 (4) (2014) 444–454.
[39] S.W. Ballinger, et al., Hydrogen peroxide- and peroxynitrite-induced mitochondrial DNA damage and dysfunction in vascular endothelial and smooth muscle cells, Circ. Res. 86 (9) (2000) 960–966.
[40] S. Da, et al., Design and synthesis of a mitochondria-targeted mimic of glutathione peroxidase, MitoEbselen-2, as a radiation mitigator, ACS Med. Chem. Lett. 5 (12) (2014).
[41] G.K. Azad, R.S. Tomar, Ebselen, a promising antioxidant drug: mechanisms of action and targets of biological pathways, Mol. Biol. Rep. 41 (8) (2014) 4865–4879.
[42] S.M. Ahwach, et al., The glutathione mimic ebselen inhibits oxidative stress but not endoplasmic reticulum stress in endothelial cells, Life Sci. 134 (2015) 9–15.
[43] X. Li, et al., Ebselen interferes with Alzheimer's disease by regulating mitochondrial function, Antioxidants 11 (7) (2022).
[44] M. Gutscher, et al., Proximity-based protein thiol oxidation by H2O2-scavenging peroxidases, J. Biol. Chem. 284 (46) (2009) 31532–31540.
[45] T. Nietzel, et al., The fluorescent protein sensor roGFP2-Orp1 monitors in vivo H(2)O(2) and thiol redox integration and elucidates intracellular H(2)O(2) dynamics during elicitor-induced oxidative burst in Arabidopsis, New Phytol. 221 (3) (2019) 1649–1664.
[46] P.N. Thai, et al., Ketone ester D-beta-Hydroxybutyrate-(R)-1,3 Butanediol Prevents decline in cardiac function in type 2 Diabetic mice, J. Am. Heart Assoc. 10 (19) (2021) e020729.
[47] W. Zhu, J.W. Smith, C.-M. Huang, Mass spectrometry-based label-free quantitative proteomics, J. Biomed. Biotechnol. 2010 (2010) 840518.
[48] S.T. Pohlack, et al., Risk variant for schizophrenia in the neurogranin gene impacts on hippocampus activation during contextual fear conditioning, Mol. Psychiatr. 16 (11) (2011) 1072–1073.
[49] R.L. Smith, et al., Analysis of neurogranin (NRGN) in schizophrenia, Am J Med Genet B Neuropsychiatr Genet 156B (5) (2011) 532–535.
[50] I. Dominguez-Gonzalez, et al., Neurogranin binds to phosphatidic acid and associates to cellular membranes, Biochem. J. 404 (1) (2007) 31–43.

[51] K. Blennow, et al., CSF neurogranin as a neuronal damage marker in CJD: a comparative study with AD, J. Neurol. Neurosurg. Psychiatry 90 (8) (2019) 846–853.
[52] L. Zhong, N.Z. Gerges, Neurogranin regulates Metaplasticity, Front. Mol. Neurosci. 12 (2019) 322.
[53] A. Garrido-Garcia, et al., Activity-dependent translocation of neurogranin to neuronal nuclei, Biochem. J. 424 (3) (2009) 419–429.
[54] Y.C. Shen, et al., Genetic and functional analysis of the gene encoding neurogranin in schizophrenia, Schizophr. Res. 137 (1–3) (2012) 7–13.
[55] H. Kvartsberg, et al., Characterization of the postsynaptic protein neurogranin in paired cerebrospinal fluid and plasma samples from Alzheimer's disease patients and healthy controls, Alzheimer's Res. Ther. 7 (1) (2015) 40.
[56] R. Tarawneh, et al., Diagnostic and Prognostic utility of the synaptic marker neurogranin in alzheimer disease, JAMA Neurol. 73 (5) (2016) 561–571.
[57] M. Xue, et al., Association of cerebrospinal fluid neurogranin levels with cognition and neurodegeneration in Alzheimer's disease, Aging (Albany NY) 12 (10) (2020) 9365–9379.
[58] L. Zhong, et al., Neurogranin enhances synaptic strength through its interaction with calmodulin, EMBO J. 28 (19) (2009) 3027–3039.
[59] K.J. Jones, et al., Rapid, experience-dependent translation of neurogranin enables memory encoding, Proc. Natl. Acad. Sci. U. S. A. 115 (25) (2018) E5805–E5814.
[60] F.J. Diez-Guerra, Neurogranin, a link between calcium/calmodulin and protein kinase C signaling in synaptic plasticity, IUBMB Life 62 (8) (2010) 597–606.
[61] M. Ordyan, et al., Interactions between calmodulin and neurogranin govern the dynamics of CaMKII as a leaky integrator, PLoS Comput. Biol. 16 (7) (2020) e1008015.
[62] S. Kumar, et al., Hydrogen peroxide decreases endothelial nitric oxide synthase promoter activity through the inhibition of Sp1 activity, DNA Cell Biol. 28 (3) (2009) 119–129.
[63] X. Zhang, et al., Hydrogen peroxide depolarizes mitochondria and inhibits IP(3)-evoked Ca(2+) release in the endothelium of intact arteries, Cell Calcium 84 (2019) 102108.
[64] J. Li, et al., Calcium entry mediates hyperglycemia-induced apoptosis through Ca(2+)/calmodulin-dependent kinase II in retinal capillary endothelial cells, Mol. Vis. 18 (2012) 2371–2379.
[65] J.M. Timmins, et al., Calcium/calmodulin-dependent protein kinase II links ER stress with Fas and mitochondrial apoptosis pathways, J. Clin. Invest. 119 (10) (2009) 2925–2941.